Capture of actinides (Th^{4+}, $[UO_2]^{2+}$) and surrogating lanthanide (Nd^{3+}) in the porous Metal-Organic Framework MIL-100(Al) from water : selectivity and imaging of embedded nanoparticles

C. Falaise,[a] C. Volkringer,[a,b] R. Giovine,[a] B. Prelot,[c] M. Huve[a] and T. Loiseau[a]

[a]Unité de Catalyse et Chimie du Solide (UCCS) – UMR CNRS 8181, Université de Lille, ENSCL, Bat C7, BP 90108, 59652 Villeneuve d'Ascq, France.

[b]Institut Universitaire de France, 1 rue Descartes, 75231 Paris Cedex 05.

[c]Institut Charles Gerhardt Montpellier UMR 5253 CNRS-UM-ENSCM Université de Montpellier, Place E. Bataillon, Bât 15, cc 1502 34095 Montpellier cedex 5, France

Supplementary information

Structural description of MIL-100(Al)

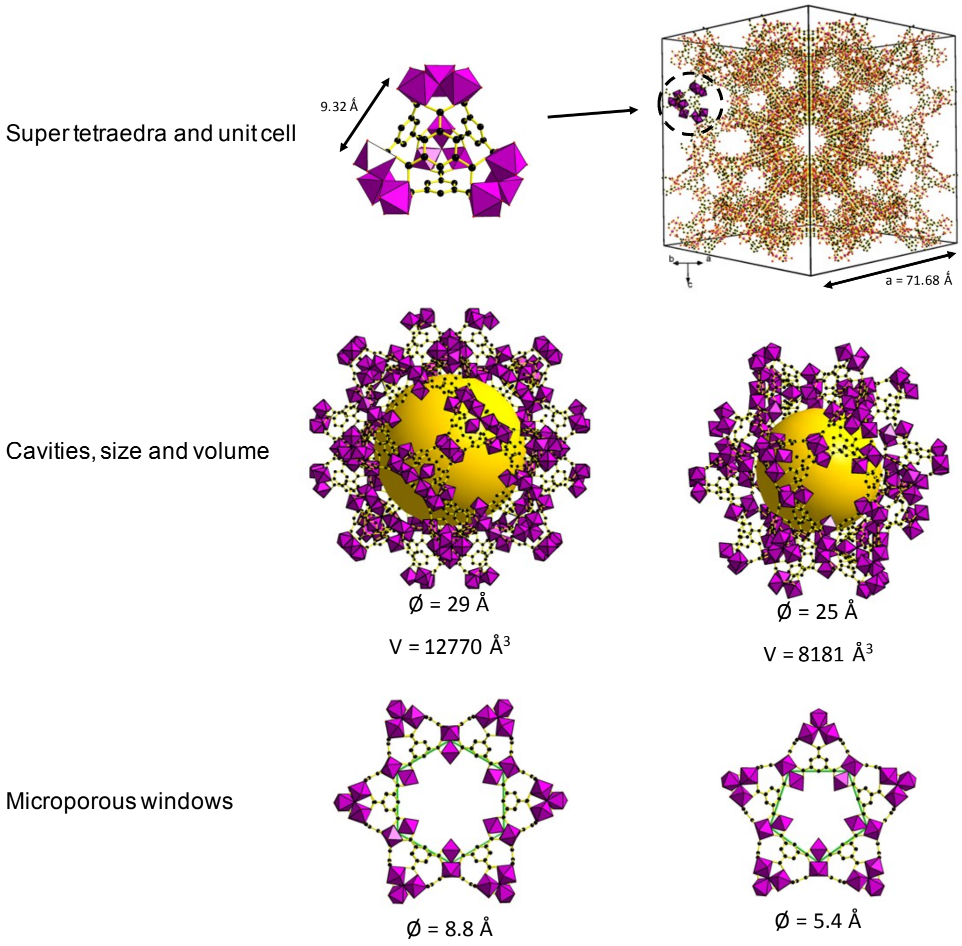

Figure S1: Structural descriptions of MIL-100(Al)

Powder X-ray diffraction

The powder X-ray diffraction patterns were collected at room temperature with a D8 advance A25 Bruker apparatus with a Bragg-Brentano geometry. The D8 diffractometer is equipped with a LynxEye detector with $Cu_K\alpha_1/\alpha_2$ radiation. The 2θ range was 3-50° with a step of 0.02° and a counting time of 0.5 seconds per step.

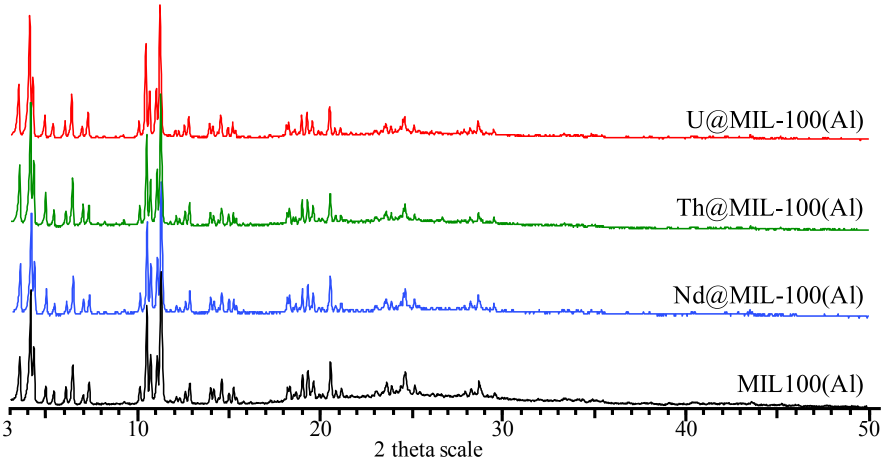

Figure S2a: Powder X-Ray diffractograms of empty and charged MIL-100(Al) without thermal treatment

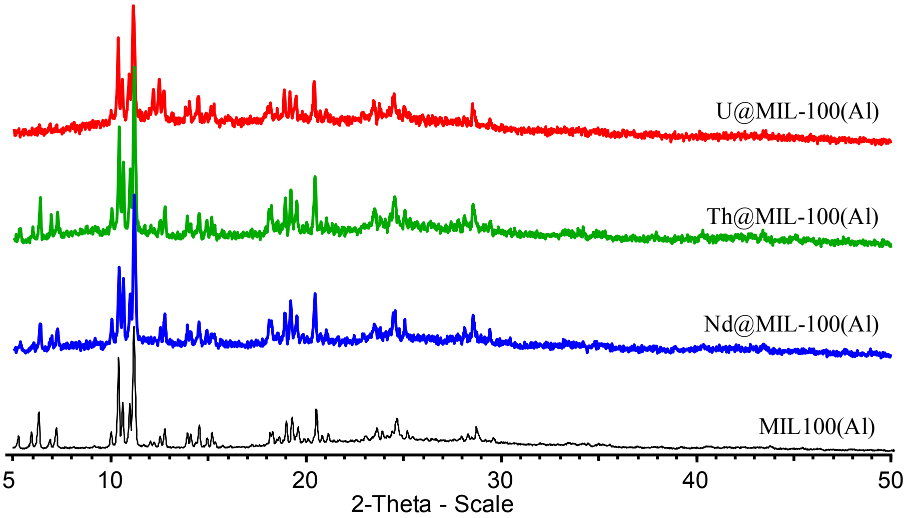

Figure S2b: Powder X-Ray diffractograms of empty and charged MIL-100(Al) after a thermal treatment at 200°C.

After the thermal treatment, the change of intensities for the low angle peaks is assigned to the dehydration of the solid.

UV-vis spectroscopy

UV/Vis spectra of the different samples have been collected by using a Perkin Elmer Lambda 650 spectrophotometer.

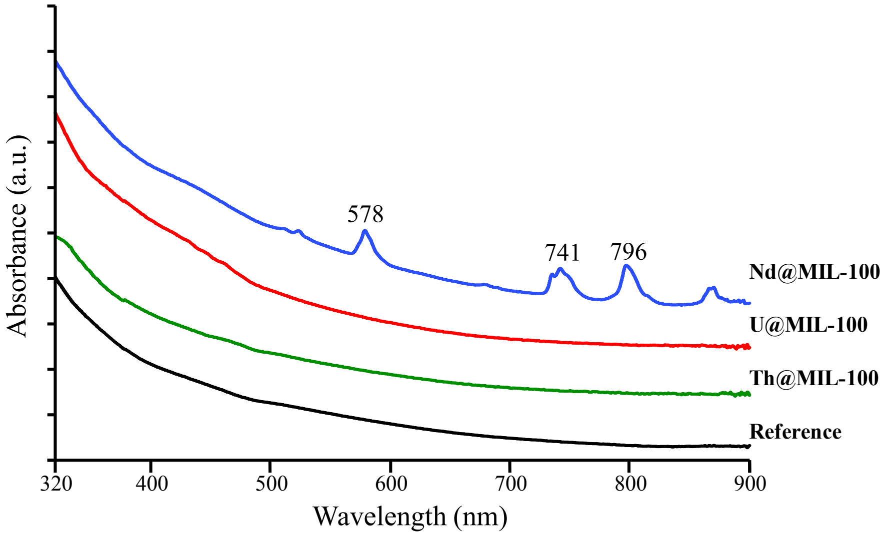

Figure S3: Solid state UV-Vis spectra of empty and charged MIL-100(Al)

Infrared spectroscopy

Infrared analysis was carried out by using a Perkin–Elmer Spectrum 2 instrument equipped with a single reflection diamond module (ATR). IR spectra were recorded in the 400–4000 cm^{-1} range with 4 cm^{-1} resolution.

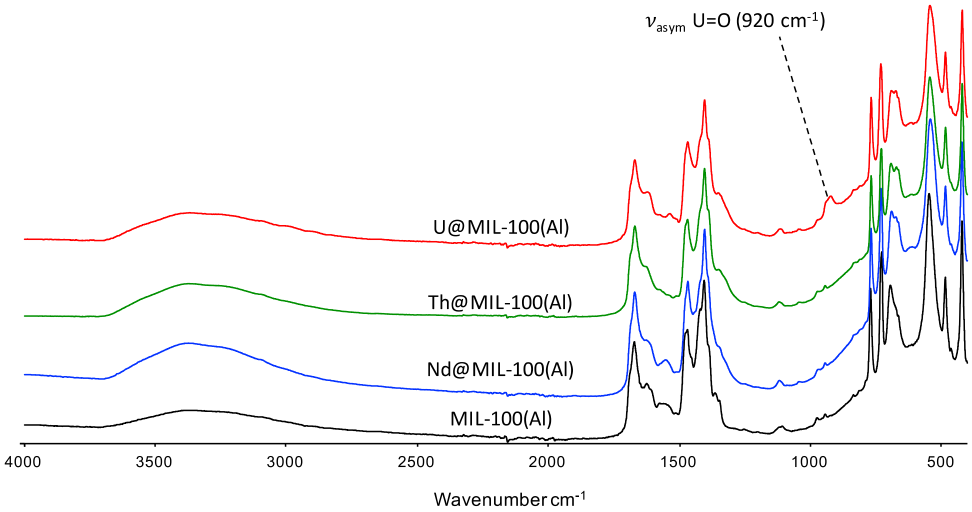

Figure S4: Infrared spectra of empty and charged MIL-100(Al)

BET analysis

Gas sorption measurements were realized using the Micromeritics ASAP 2020 apparatus. Before gas sorption, the sample was activated at 200°C under vacuum overnight. The porosity of the sample was estimated by gas sorption isotherm experiment in liquid nitrogen (77K). For surface area calculation, BET model was applied in the 0.01-0.2 p/p_0 range.

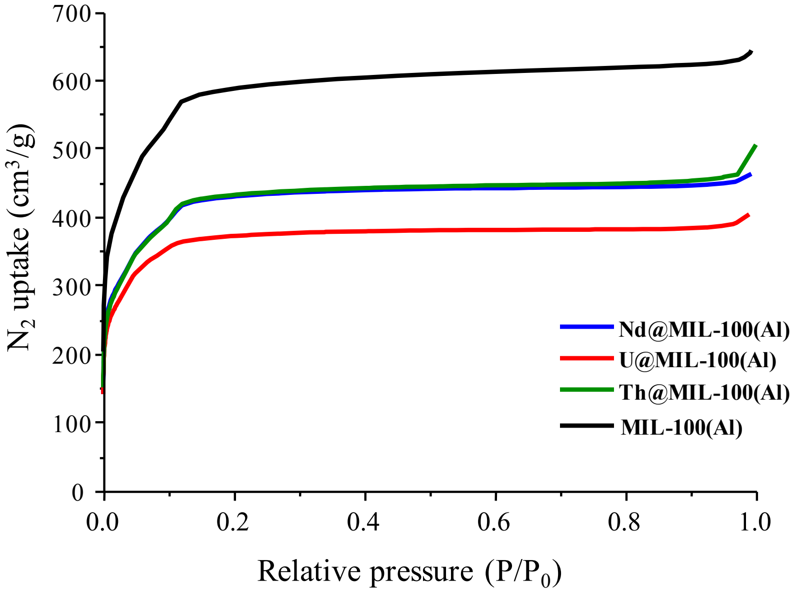

Figure S5: Nitrogen adsorption isotherm (77K) of empty and charged MIL-100(Al)

Sorption experiments

Sorption of $[UO_2]^{2+}$ cations at various temperatures

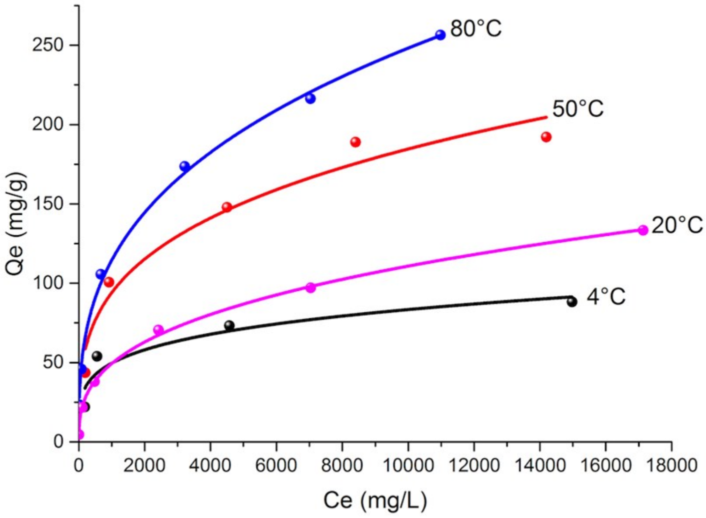

Figure S6: Experimental $[UO_2]^{2+}$ sorption isotherm collected at 4, 20, 50 and 80°C, fitted with Freundlich model (straight line).

Sorption of $[UO_2]^{2+}$ cations at various pH

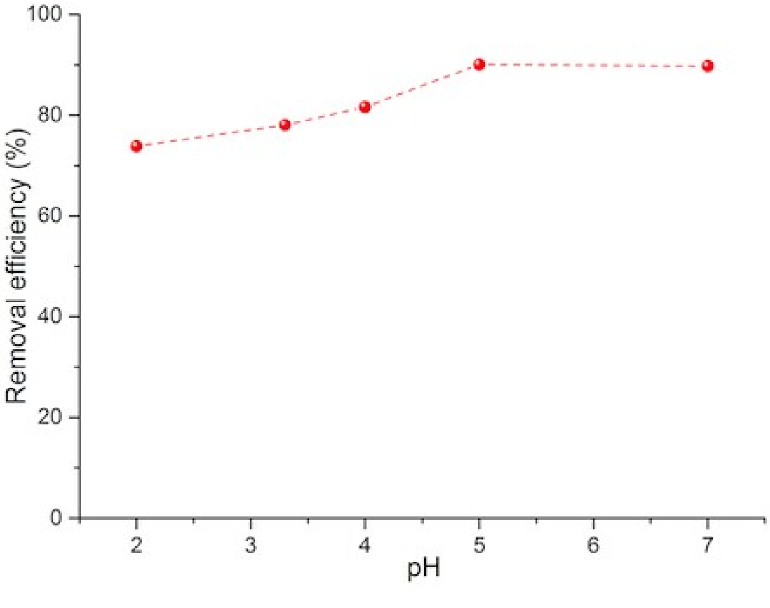

Figure S7: Removal efficiency of $[UO_2]^{2+}$ in MIL-100(Al) at different pH values ranging from 2 to 7.

Removal efficiency

The removal efficiency was calculated by using the following equation.

$$Removal\ (\%) = \frac{(C_i - C_{e(or\ t)})}{C_i} \times 100$$

Where C_t and C_e are the concentration at time *t* and at equilibrium (mg/l), C_i is the initial concentration of cation (mg/l), q_t and q_e are the amount adsorbed at time *t* and equilibrium (mg/g).

Pseudo first order kinetic model

The linear form of pseudo first order kinetic model is expressed by the following equation.

$$\log (q_e - q_t) = \log q_e - \frac{k_1}{2.303} t$$

Where q_e and q_t are previously defined, k_1 is the pseudo first order rate constant for the adsorption process (min^{-1}).

Table S1: Parameters of the pseudo-first order kinetic model extracted from experimental data of Nd^{3+}, Th^{4+}, $[UO_2]^{2+}$ kinetic sorptions in MIL-100(Al)

	q_e exp. (mg/g)	**r²**	**q_e calc. (mg/g)**	**k_1 (min^{-1})**
Nd^{3+}	53	0,989	38	0,10
Th^{4+}	112	0,959	62	0,17
UO_2^{2+}	96	0,881	31	0,14

Pseudo second order kinetic model

The linear form of pseudo second order kinetic model is expressed by the following equation.

$$\frac{t}{q_t} = \frac{1}{k_2 {q_e}^2} + \frac{1}{q_e} t$$

Where q_e and q_t are previously defined, k_2 is the pseudo second order rate constant for the adsorption process (g/mg min).

Table S2: Parameters of the pseudo-second order kinetic model extracted from experimental data of Nd^{3+}, Th^{4+}, $[UO_2]^{2+}$ kinetic sorptions in MIL-100(Al)

	q_e exp. (mg/g)	**r²**	**q_e calc. (mg/g)**	**k_2 (mg.g^{-1}.min^{-1})**
Nd^{3+}	53	0,998	56	5,8 x 10^{-3}
Th^{4+}	112	0,999	115	13,5 x 10^{-3}
UO_2^{2+}	96	0,999	97	5,5 x 10^{-3}

Intra-particle diffusion model

The linear form of pseudo second order kinetic model is expressed by the following equation.

$$q_t = k_i t^{1/2} + C$$

Where q_e, q_t and t are previously defined, k_i is the pseudo second order rate constant for the adsorption process (g/mg min) and C is the intercept (mg/g).

Table S3: Parameters of the intraparticle kinetic model extracted from experimental data of Nd^{3+}, Th^{4+}, $[UO_2]^{2+}$ kinetic sorptions in MIL-100(Al)

	r^2	**C. (mg/g)**	**k_i (mg.g^{-1}.min$^{-0,5}$)**
Nd^{3+}	0,82	17	5,4
Th^{4+}	0,62	64	8,0
UO_2^{2+}	0,61	62	5,5

Langmuir and Freundlich isotherms

The equation of Langmuir is expressed by the following equation.

$$q_e = \frac{k_L C_e}{1 + a_L C_e}$$

Where q_e and C_e are previously defined, k_L (l/g) and a_L (l/mg) are the Langmuir isotherm constants.

The equation of Freundlich is expressed by the following equation.

$$q_e = k_F C_e^{1/n_F}$$

Where q_e and C_e are previously defined, k_F (l/g) and a_F (l/mg) are the Freundlich isotherm constants.

Table S4. Parameters of the Langmuir and Freundlich isotherm models extracted from experimental adsorption isotherms data Nd^{3+}, Th^{4+}, $[UO_2]^{2+}$ isotherm sorptions in MIL-100(Al)

	Langmuir			**Freundlich**		
Cation	**r^2**	**k_L(L/g)**	**a_L (L/mg)**	**r^2**	**k_F (L/g)**	**n_F**
Th^{4+}	0,921	0,286	$1{,}6 \times 10^{-3}$	0,985	11,76	3,47
UO_2^{2+}	0,937	0,071	$5{,}2 \times 10^{-4}$	0,997	4,36	2,84
Nd^{3+}	0,991	0,015	1×10^{-4}	0,981	0,15	1,49

Isotherm Titration Calorimetry (ITC).

The enthalpy changes accompanying the ion adsorption at 298 K were measured by means of a TAM III multi-channel microcalorimetric system (TA Instruments) described previously [1-2]. The 1 mL measuring ampoule containing about 10 mg of MIL-100(Al) powder for Nd^{3+} and UO_2^{2+}, or 40 mg for Th^{4+}, suspended in 0.8 mL of ultrapure water was placed in the microcalorimeter. The homogeneity of the solid suspension was maintained by means of an agitation system equipped with a Gold paddle stirrer (90 rpm). The reference ampoule is filled with the same amount of ultrapure water. Pulse injections of an appropriate stock solution (150 mmol L^{-1} Nd^{3+}, or Th^{4+}, 140 mmol L^{-1} $[UO_2]^{2+}$) were performed. Successive injections of the 10 µL aliquots of the cation solution during 10 sec resulted in an heat effect due to sorption processes. The signal was recorded with an equilibration time of 2 or 3 hours applied between 2 injections, in the direct heat flow mode. The experimental enthalpy changes were subsequently corrected for dilution effects. The dilution experiments were carried out under the same experimental conditions but without introducing any solid into the sample ampoule. Further procedures for data processing were described previously [1, 3]. The measurements were repeated at least three times.

References

1. Prelot, B.; Ayed, I.; Marchandeau, F.; Zajac, J., On the real performance of cation exchange resins in wastewater treatment under conditions of cation competition: the case of heavy metal pollution. *Environmental science and pollution research international* **2014,** *21* (15), 9334-43.
2. Thach, U. D.; Hesemann, P.; Yang, G.; Geneste, A.; Le Caër, S.; Prelot, B., Ionosilicas as efficient sorbents for anionic contaminants: Radiolytic stability and ion capacity. *Journal of Colloid and Interface Science* **2016,** *482*, 233-239.
3. Zajac, J., Calorimetry at the Solid–Liquid Interface. In *Calorimetry and Thermal Methods in Catalysis*, Auroux, A. E., Ed. Springer Series in Materials Science: 2013; pp 197-270.